Bulletin of Engineering Geology and the Environment (2021) 80:3023–3040
https://doi.org/10.1007/s10064-021-02134-4

ORIGINAL PAPER

# Evaluating the influence of engineering geological parameters on TBM performance during grinding process in limestone strata

Seyed Mahdi Pourhashemi[1] · Kaveh Ahangari[1] · Jafar Hassanpour[2] · Seyed Mosleh Eftekhari[3]

Received: 16 August 2020 / Accepted: 6 February 2021 / Published online: 18 February 2021


## Abstract

The chipping and grinding processes are the basis for understanding rock cutting during TBM excavation in hard rock conditions. The chips are produced when tensile fractures created by adjacent cutters propagate parallel to the tunnel face and coalesce whereas grinding occurs when fractures do not fully propagate through the rock and only fines are generated. Chipping is the normal and efficient boring process using machines equipped with disc cutters. Consequently, almost all of the models proposed for predicting the TBM penetration have been developed by the assumption that chipping is the dominant mode. It is obvious that these models are unable to predict correctly TBM performance when grinding is dominated in the rock cutting process. In this study, the relationships between engineering geological properties of the rock units (Cretaceous limestones) and operating and performance parameters of a refurbished EPB-TBM, employed for completion of SEL6 (the Southern Extension of Line 6, Tehran Metro) tunnel, were evaluated and analyzed. In this project due to limitations in the load capacity of the employed cutters and insufficient initial penetration in rock, the excavation was mostly carried out on grinding-dominated mode. So, the suitable data for establishing a special database and consequent analyses were provided. The established database composed of actual operating and performance parameters of the machine (i.e., cutterhead penetration and RPM and cutter load) and also engineering geological properties (i.e., UCS, alpha angle, GSI, and RQD) of limestone strata. Finally, by statistical analyses performed on collected and screened data (41 data sets), some simple, site-specific, empirical equations were developed to predict the TBM performance on grinding mode. In addition, according to the multivariate regression method, a significant relationship between the cutterhead penetration (PRev), the cutter load (Fn), intact rock strength (UCS), and geological strength index (GSI) was established, statistically. The obtained results demonstrate that this engineering geological-based model could provide a new applicable equation for accurately predicting TBM performance for similar geological conditions where grinding is dominant.

**Keywords** Tunnel boring machine · Penetration · Grinding · Chipping · Rock mass parameters

## Introduction

One of the important issues for estimating construction time and cost of mechanized tunnels is the accurate prediction of TBM performance parameters, notably the penetration rate. During the past few decades, several empirical models have been developed for the prediction of TBM penetration rate by analyzing the interaction between the engineering geological properties of rock and the operating parameters of the TBM (Yagiz 2008; Gong and Zhao 2009; Hassanpour et al. 2011, 2015, 2020; Farrokh et al. 2012, Delisio et al. 2013; Koopialipoor et al. 2019; Lazemi and Dehkordi 2019; Zhou et al. 2020) as summarized in Table 1.

As presented in Table 1, the empirical models are mainly based on measured data of engineering geological properties of intact rock and rock mass (i.e., uniaxial compressive strength (UCS), rock-quality designation (RQD), rock mass rating (RMR), and geological strength index (GSI)) and TBM operating parameters collected continuously during tunnel excavation. It was reported in Table 1 that correlations between the measured engineering-geological properties and TBM operation parameters are defined by statistical analysis (Yagiz

✉ Jafar Hassanpour
hassanpour@ut.ac.ir

[1] Department of Mining Engineering, Science and Research Branch, Islamic Azad University, Tehran, Iran

[2] School of Geology, College of Science, University of Tehran, Tehran, Iran

[3] Department of Mining Engineering, Faculty of Engineering, Tarbiat Modares University, Tehran, Iran

**Table 1** Review of empirical predictive models for TBM performances

| Prediction value | Reference | Engineering geological properties | TBM operation parameters | Analysis methods |
|---|---|---|---|---|
| ROP (m/h) | Yagiz (2008) | α, intact rock uniaxial compressive strength (UCS), average distance between planes of weakness (DPW) | | Statistical analysis |
| Boreability Index (BI) (kN/mm/rev) | Gong and Zhao (2009) | Intact rock uniaxial compressive strength (UCS), BI, volumetric joint count (Jv), and α | Cutter force | Statistical analysis |
| Field Penetration Index FPI (kN/mm/rev) | Hassanpour et al. (2011, 2015, 2020) | RQD and intact rock uniaxial compressive strength (UCS) | Cutter force, RPM | Statistical analysis |
| Penetration per revolution PRev (mm/rev) | Farrokh et al. (2012) | Tunnel diameter, rock type numerical, intact rock uniaxial compressive strength (UCS), RQD, and disc cutter normal force | Revolution per minute (RPM) and disc cutter normal force | Statistical analysis |
| Field Penetration Index for blocky rock conditions, $FPI_{blocky}$ | Delisio et al. (2013) | Volumetric joint count (Jv) and the intact rock uniaxial compressive strength (UCS) | Cutter force, RPM | Statistical analysis |
| Advance rate—AR (m/h) | Zhou et al. (2020) | Brazilian tensile strength (BTS), RPM, RQD, TF, intact rock uniaxial compressive strength (UCS), RMR | Thrust force (TF) and revolution per minute (RPM) | Genetic programming approaches |
| Penetration per revolution (mm/rev) | Lazemi and Dehkordi (2019) | Absolute value of the drop modulus ( \|M\| ) | Equivalent thrust per cutter (Meq) | Statistical analysis |
| Penetration rate, PR (m/h) | Koopialipoor et al. (2019) | RQD, intact rock uniaxial compressive strength (UCS), RMR, Brazilian tensile strength (BTS) | Cutterhead thrust force (TF), revolutions per minute (RPM) | Neural network models |

2008; Gong and Zhao 2009; Salimi et al. (2018); Hassanpour et al. 2011, 2015, 2020; Farrokh et al. 2012; Delisio et al. 2013; Koopialipoor et al. 2019; Lazemi and Dehkordi 2019) and Computer-Aided Models (i.e., neural network models and genetic programming approaches) (Koopialipoor et al. 2019; Zhou et al. 2020).

The empirical models have great importance during the early stages of tunneling and design works since this is a more practical method as compared with extensive and expensive experimental solutions (Yagiz 2008). On the one hand, the empirical models offer the greatest correspondence with the reality, but on the other hand, the proposed correlations are strongly dependent on the TBM specifications and ground conditions of the case study (Farrokh et al. 2012; Brino et al. 2015; Armetti et al. 2018). In other words, the empirical models are site-specific in terms of the geological conditions along the tunnels.

In addition, one important shortcoming in almost all of the proposed models is that they have been developed with assumption that chipping occurs during rock cutting process. However, in some cases, due to high strength of rock and/or insufficient load of cutter, chipping phenomenon beneath the cutters is not complete.

The cutting process in hard rock for a tunnel boring machine involves roller disc-cutters applying cyclical pressure on concentric rings in tunnel face with fragmentation occurring between disc cutters' paths (Fig. 1a). Recent studies by M. Villeneuve (2008), C. Frenzel et al. (2012), MC. Villeneuve et al. (2012), and MC. Villeneuve (2017) explained the difference of chipping and grinding modes and concluded that the chipping process is the basis for understanding rock cutting during TBM tunneling and is postulated to be accomplished by inducing tensile fractures and cracks into the rock mass, which then propagate parallel to the tunnel face.

Rock failure mechanism during excavation with a disc cutter is illustrated in Fig. 1a. A crushed zone develops beneath the disc cutter as it is forced into the rock (Balci and Bilgin 2007; Labra et al. 2017). The fractures and cracks induced into the rock act to precondition the rock, making it easier to cut during subsequent rotations of the TBM cutterhead, while the fractures and cracks propagating parallel to the tunnel face will colligate with similar fractures and cracks induced by adjacent disc cutters to create the rock cuttings called chips.

Grinding occurs when fractures do not propagate through the rock effectively, and only fine rock cuttings are generated. So, muck size distributions are very different in grinding and chipping conditions. Figure 2 shows an overview of excavated rock size distributions from the different TBM projects in Europe, where excavation has occurred in chipping conditions (Berdal et al. 2018). In order to compare generated rock cuttings in grinding and chipping, a typical

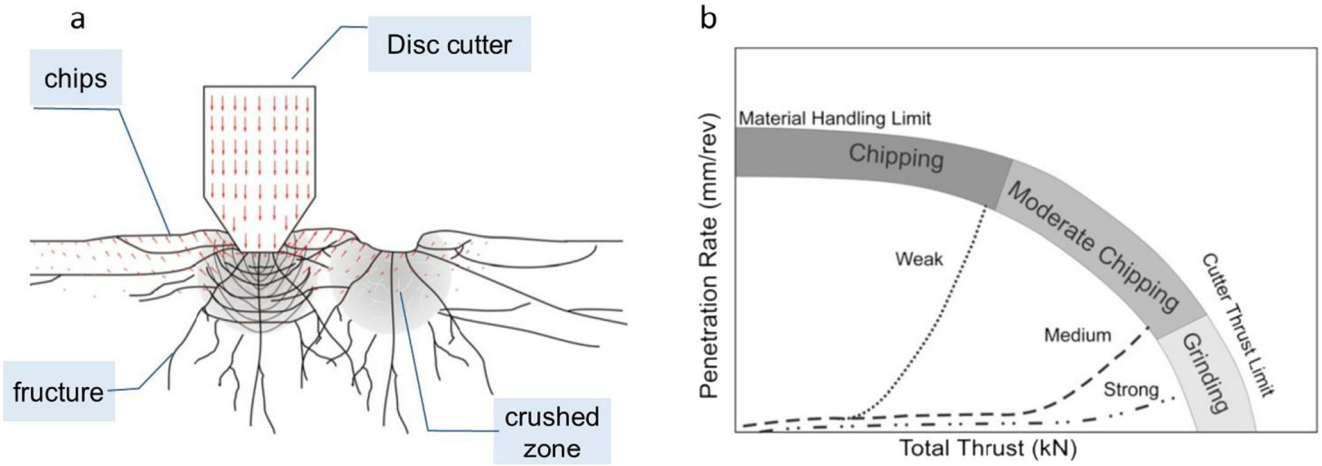


**Fig. 1** **a** Schematic cross section of TBM disc cutter and tunnel face showing boring process; **b** penetration versus thrust graphs and regions of grinding and chipping performance (Villeneuve et al. 2012)

muck size distribution curve from the SEL6 project, where the grinding phenomenon was dominant, was also added to Fig. 2. As shown, the excavated materials in the SEL6 project are very finer than the muck created in other projects.

Traces of disc cutter rotations as well as created ridges and grooves, in tunnel faces of Uma Oya (Sri Lanka) and SEL6 projects, are illustrated in Figs. 3 and 4, respectively. As shown in these figures, grooves in grinding conditions are deeper than chipping-dominated conditions. The reason for this could be related to the cutting mechanism in these processes. When grinding is dominated in the rock cutting process, fractures do not propagate through the rock, deep kerfs are formed beneath the disc cutters, and large ridges remain between two adjacent grooves. Also, a large quantity of rock powder particles and small grains are generated. In contrast, in chipping-dominated mode, the rock is cut midway between the two kerfs and also sideways. Rock debris is rarely produced, and only a small amount of fine rock powder particles are generated. Therefore, kerf depth on a rock face in the grinding condition is dipper than chipping.

Efficient penetration, as a function of the load, was applied to the disc cutters, and the resulting penetration relies on ensuring that a chipping mechanism dominates over a crushing under the disc cutter of TBM (Fig. 1a). As shown in Fig. 1b, efficient cutter penetration, as a function of thrust (cutter load), relies on ensuring that a chipping mechanism dominates over a crushing mechanism beneath the cutters. The most important factors influencing cutting efficiency are the cutter load, engineering geological properties (e.g., UCS, RQD, and discontinuity spacing) and initial penetration. The relationships between the intact rock strength, disc cutter thrust force (cutter load), and penetration were very well introduced by C. Frenzel et al. (2008) and are shown in Fig. 5a. As shown, practically, when cutter load is not sufficient (less than 150 kN in weaker rocks), grinding is the dominant phenomenon in rock cutting process. Field studies in similar projects have shown that a

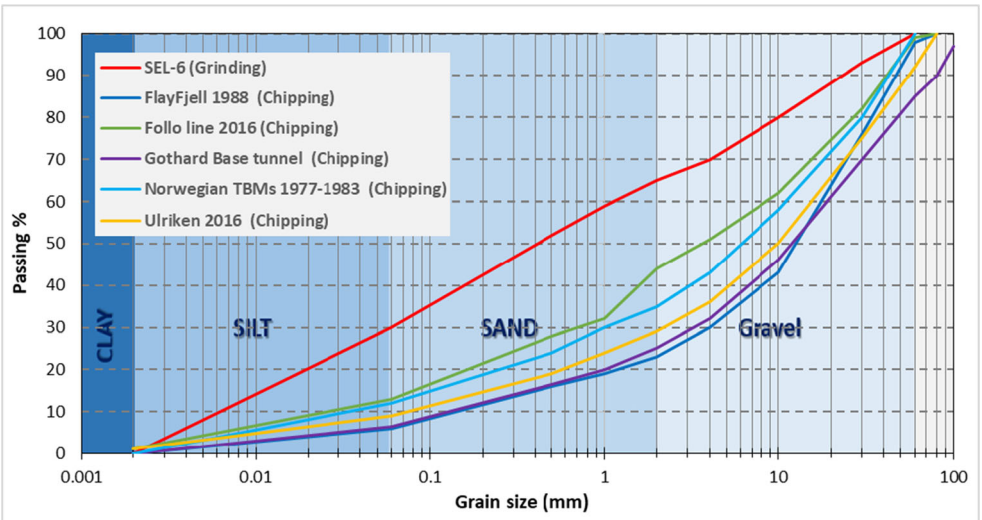


**Fig. 2** Excavated rock size distributions from various hard rock TBM projects in Europe (chipping conditions) and their comparison with muck size distribution in SEL6 project (grinding condition)

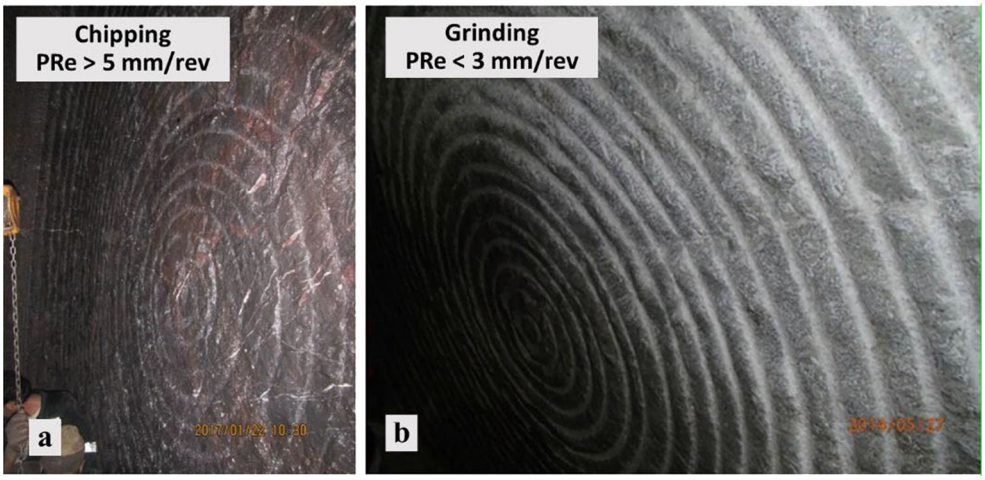


**Fig. 3** Two views of tunnel face in Uma Oya project, Sri Lanka; **a** chipping-dominated mode and **b** grinding-dominated mode

cutterhead penetration (PRev) of more than 4–5 mm/rev is required for chipping phenomenon to occur completely.

As shown in Fig. 5b, the previous studies have almost exclusively focused on penetrations bigger than 4–5 mm/rev, where a chipping mechanism dominates, whereas this study emphasizes grinding dominated excavation.

As noted above, previous empirical models for predicting TBM performance were limited to the chipping mode. Furthermore, since excavation in grinding mode may impact TBM performance, a need for an improved penetration predictive model for TBMs operating in grinding conditions became evident. Therefore, in this study, attempts were made to develop a new empirical model based on the comparison between the engineering geological properties and the TBM performance data collected during the excavation of the Southern Extension of Line 6, Tehran Metro.

## Description of the analyzed tunnel project

The SEL6 (Southern Extension of Line 6) tunnel, with a total length of 6 km and a boring diameter of 9.2m, is an extension of the Tehran metro line 6 (Fig. 6) in an area where Cretaceous limestone rock masses outcrop in the middle of Tehran alluviums (Fig. 7). As shown in Fig. 8, Tehran metro line 6 project with a length of 38 km and 31 stations is the longest metro line in Iran that has been constructed between Dolat-Abad, at South-east, and Shahran, at North-west of Tehran, by TBM

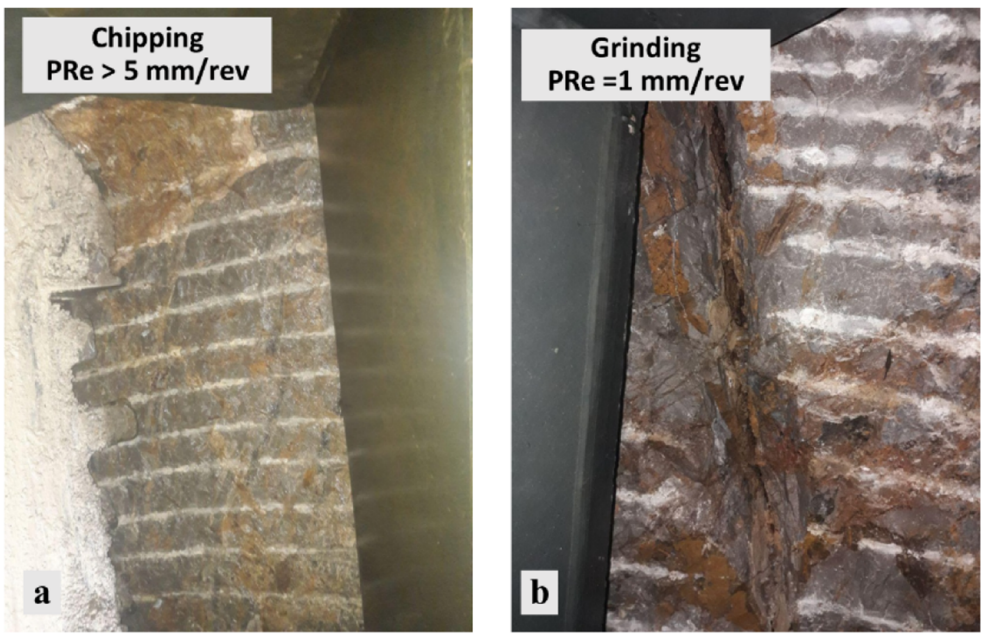


**Fig. 4** Two views of tunnel face in SEL6 project. **a** Chipping-dominated mode and **b** grinding-dominated mode

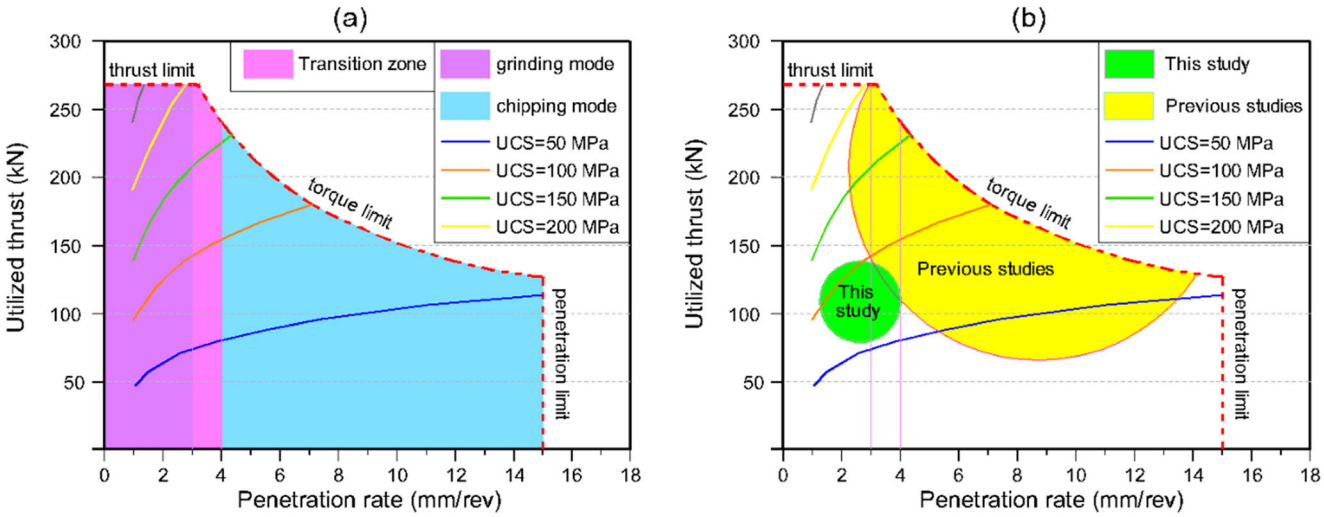


**Fig. 5** **a** Operating limits of a TBM at different rock strengths (modified from Frenzel et al. 2008). **b** Thrust-penetration database including previous studies presented in Table 1 (yellow area) and this study model (green area)

and NATM methods (Tarigh Azali et al. 2018). The SEL6 tunnel has been designed to be completed using a refurbished EPB-TBM (originally designed to work in soft ground condition). The boring was started from the Northern (Dolat-Abad) portal in 2017 and has not been finished yet. These excavations are all shallow with typical depths to the tunnel crown of between 15 and 30 m. The bored section of SEL6 tunnel has passed through two different geological formations, namely, Quaternary Alluviums of Tehran and Cretaceous limestone rocks.

## Regional geological setting

Tehran is located in the southern front of the Alborz Mountain ranges, a tectonically active region between the Caspian Sea and Iran plateau. The Tehran region is bounded to the north by the

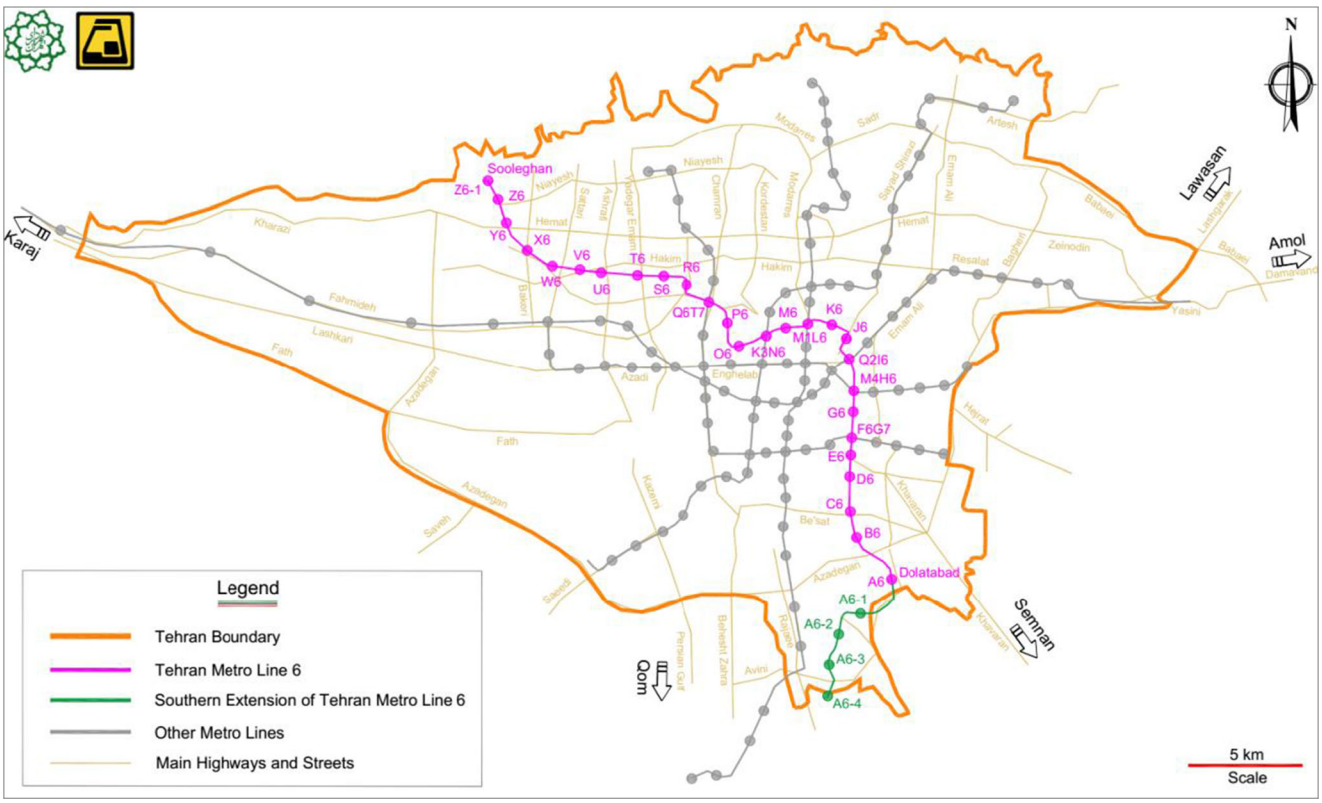


**Fig. 6** Location of line 6 of Tehran Metro and its southern extension (SEL6 tunnel) on Tehran map

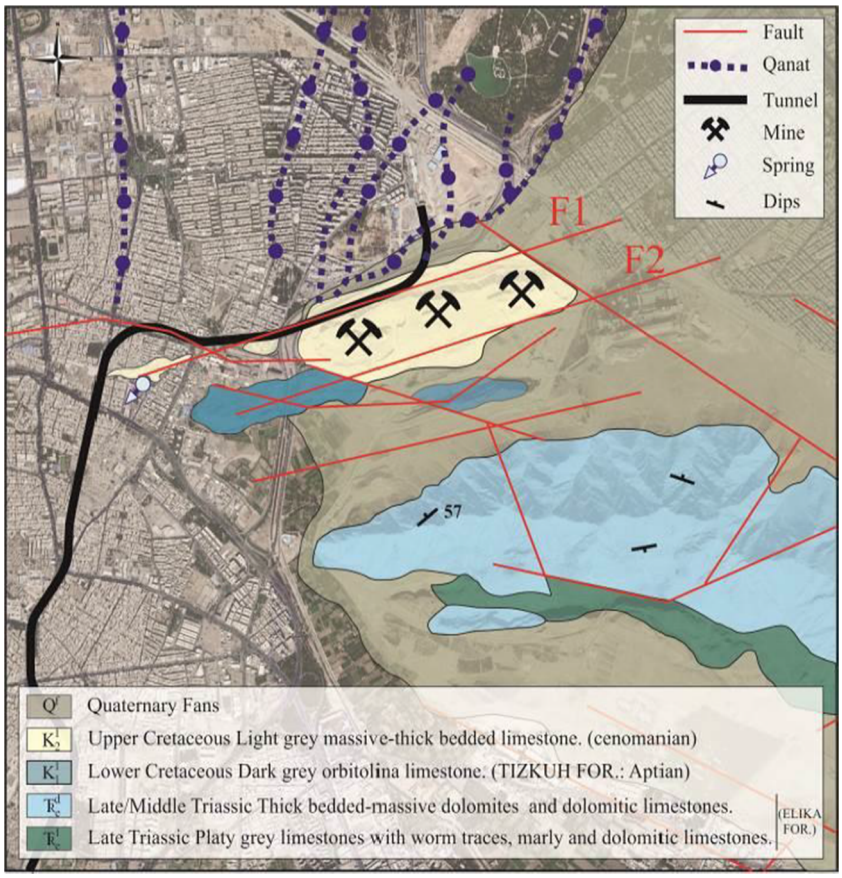


**Fig. 7** Geological map of SEL6 tunnel (Firouzei et al. 2019)

Alborz Mountains, to the southeast by mounts Bibi-Shahrbanoo and Sepahieh. Tehran is divided into three structural and stratigraphic zones including the northern mountains, eastern and southern mountains, and the Tehran plain (Tarigh Azali et al. 2013). According to Tarigh Azali et al. (2013), the Tehran plain mainly consists of quaternary formations, which are often the result of erosion and redeposition of former sediments. The plain extends to the south as a young fan and generally composed of unsorted fluvial and river deposits. The effects of climatic processes as well as recent tectonic activities have caused alluvium of various types, thicknesses, and grain sizes. Mount Bibi-Shahrbanoo, is exposed as some hills, is located in the southeast of Tehran, in the eastern margin of Shahr-e-Rey. The hills are a continuation of the mount Bibi-Shahrbanoo toward the inner part of the city. The hills are composed of the dolomite and limestone belonging to the Triassic and Cretaceous geological periods, ranging from medium-bedded to massive rocks with the color of light brown and gray.

## SEL6 tunnel geology

A geological map and a longitudinal geological section of the SEL6 tunnel are shown in Figs. 7 and 8, respectively. As shown in these figures, SEL6 tunnel excavated by TBM is located in two distinct tectonic formations called Tehran alluvium and Cretaceous limestone. These are, respectively,

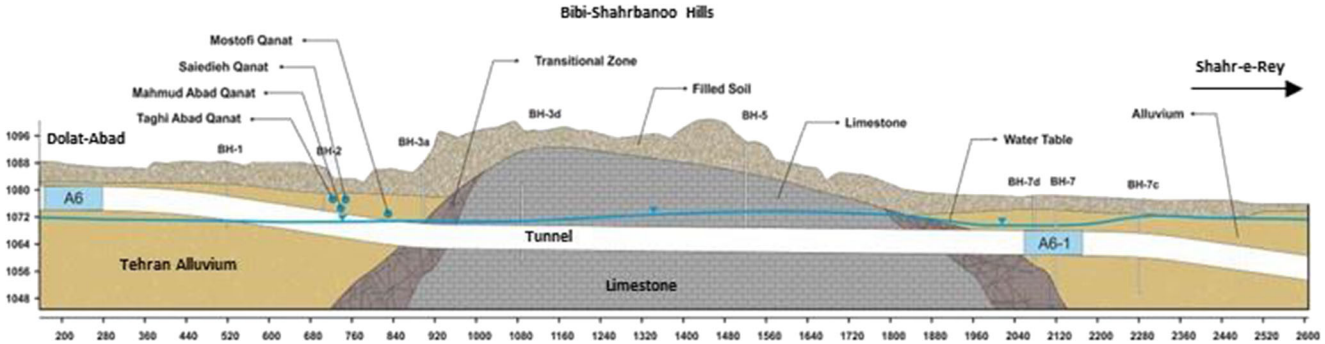


**Fig. 8** Longitudinal geological section along the SEL6 tunnel (From chainage 0+200 to 2+600) (Firouzei et al. 2019)

composed of fine-grain soil and strong limestone rocks. As presented in Fig. 8, moving from the north (left) to the south (right), the first part of the tunnel is intersected by a zone of fine-grain soil unit which precedes the northern part of the Bibi-Shahrbanoo hills. After around 800 m from the Dolat-Abad portal, the tunnel pass through Upper Cretaceous rocks, mainly composed of medium to thick-bedded limestone (Rahsaz-Tarh Consulting Engineers 2016). Figure 9 shows the outcrops of the limestone, which were observed during geological field surveys. The two contacts between limestone layers and the alluviums are composed of mixed soil and blocky rock called the transitional zone.

**Table 2** Specifications of employed TBM

| TBM parameters | Value |
|---|---|
| Bore diameter (mm) | 9190 |
| Machine type | EPB |
| Cutters' diameter (inch) | 17 |
| Number of disc cutters (double ring) | 26 |
| Cutting knives | 164 |
| Buckets | 16 |
| Power (kW)—electric motor | 2400 |
| Cutterhead torque (nominal) (kNm) | 17,197 |
| Working pressure (bar) | 3 |
| TBM weight (approx.) (ton) | 650 |

## Machine specifications

The main features of the Herrenknecht earth pressure balance TBM used for the excavation of the SEL6 tunnel are presented in Table 2, and a picture of the machine in factory is shown in Fig. 10.

The preliminary route of the tunnel was composed of alluvium and soft ground, geologically. Generally, TBM is designed based on the given and dominant site ground conditions. In other words, the geological conditions determine the type and position of the excavation tools on the TBM cutterhead. According to geological conditions of the preliminary tunnel route, double-cutters were chosen and were installed on cutterhead as the cutting tool. But, because of environmental and traffic limitations, the SEL6 tunnel route was changed. The engineering geological studies revealed that more than 1200 m of the new route is composed of limestone rocks, although the cutterhead was built for soft ground and equipped with double-cutters. As shown in Fig. 10, the TBM is equipped with 26 double-cutters with 17-inch rings.

A double-cutter is composed of two rings but has only one bearing. According to design criteria, for 17-inch cutter, every bearing can carry up to 270 kN. Therefore, during excavation, the machine operator cannot apply force more than 135 kN on

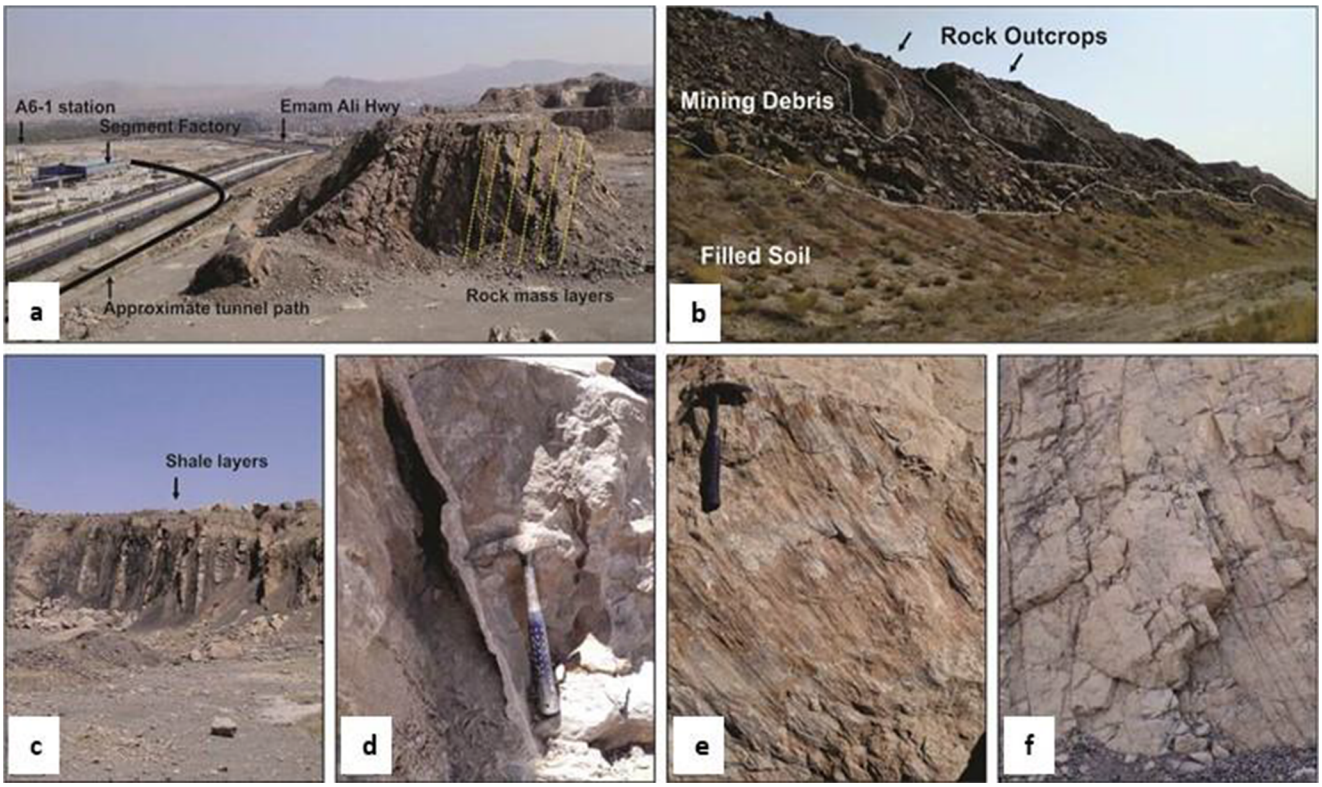


**Fig. 9** **a** Tunnel path and workshop from the mining site, **b** outcrops of rock covered by mining debris and filled soil, **c** alternation of shale and limestone layers, **d** joint with opening, **e** mirror fault, and **f** blocky rock (Rahsaz-Tarh Consulting Engineers 2016)

**Fig. 10** TBM machine used in the excavation of SEL6 tunnel

every ring. In other words, each ring cannot practically apply more than 135 kN into the rock which is not sufficient to create penetration higher than 5 mm/rev.

In this project, where the cutting load applied by disc cutter was inadequate for penetrating into rock, the chipping process practically became incomplete and the grinding process was the dominant phenomena. Therefore, this project provided an opportunity to investigate the relationship between cutterhead penetration and engineering geological characteristics of limestone in grinding conditions.

## Development of a database

In this study, to analyze the TBM performance in limestone rock units, a comprehensive database was established. The database is composed of two main parts. The first one includes machine operating parameters (such as applied thrust force, cutter load, RPM, torque, cutterhead penetration, penetration rate, and boring time) that were recorded continuously by the TBM acquisition system during tunneling. These parameters were averaged for all of the 1.5m installed rings. The second part comprises engineering-geological parameters of rock mass and intact rock obtained from extensive site investigations. The site investigation included a detailed tunnel face mapping of the rock mass, muck assessment and sampling, rock coring, and laboratory tests. In order to continuously log the various rock mass conditions encountered by TBM, the tunnel face mapping and rock sampling were frequently conducted (Fig. 11).

During the excavation, tunnel face mapping, muck sampling, and rock core sampling at the same tunnel face were carried out about once per 10–50 m when the machine stopped for cutterhead inspection and cutter replacement. More than 40 tunnel faces were mapped in the SEL6 tunnel during tunneling. The rock mass conditions varied from fresh limestone rock masses to highly fractured and moderately weathered rock masses. Usually, the measured and recorded parameters in the tunnel face mapping included lithology, rock weathering grade, type of discontinuities (i.e., joints, faults, veins, and bedding), and their properties, as orientation, spacing and surface condition (following ISRM (1978)), and also the angle between the tunnel axis and the discontinuity plane and RQD and geological strength index (GSI).

To collect samples for laboratory tests, as point load tests (Fig. 12b), UCS, and petrographic analysis, the core samples were taken by portable drilling machine during tunnel face mapping (Fig. 12a). Finally, these data were specified to the corresponding 1.5m rings.

Most important engineering geological properties of the rock masses and the TBM operating parameters are described and statistically analyzed in the following.

### Orientation of discontinuities in rock masses

Experiences show that joint orientation has crucial importance on the performance of TBM. Usually, the surrounding rock mass of the tunnel contains 2–3 major sets of discontinuities plus some random joints. Each discontinuity set, depending on its orientation, may have different effects on the TBM penetration. On the other hand, the higher the discontinuity density or frequency, the larger the effect of the discontinuities on the TBM penetration. To be able to quantify the influence of discontinuity orientation on the cutterhead penetration, the alpha angle ($\alpha$) that is the angle between the tunnel axis and the panes of the discontinuity plane can also be determined from the tunnel face mapping. The alpha ($\alpha$) in degrees can be calculated using the following equation (Bruland 1998):

$$\alpha = \arcsin\left(\sin\alpha_f \times \sin(\alpha_t - \alpha_s)\right), \quad (1)$$

where $\alpha_f$ and $\alpha_s$ are respectively the dip and strike of encountered planes of discontinuity in the rock mass and $\alpha_t$ is the direction of the tunnel axis in degrees. The histogram and the descriptive statistical analysis of the alpha angle ($\alpha$) gathered during excavation and recorded in the database are presented in Fig. 13a and Table 3, respectively.

### Intact rock strength

Uniaxial compressive strength (UCS) is commonly used to assess the rock mass boreability (Gong and Zhao 2009; Armetti et al. 2018, Hassanpour et al., 2015); moreover, as observed in the Table 1, the predictive models of TBM performance mainly involve UCS as an input parameter. In this study, UCS values have been determined using point load

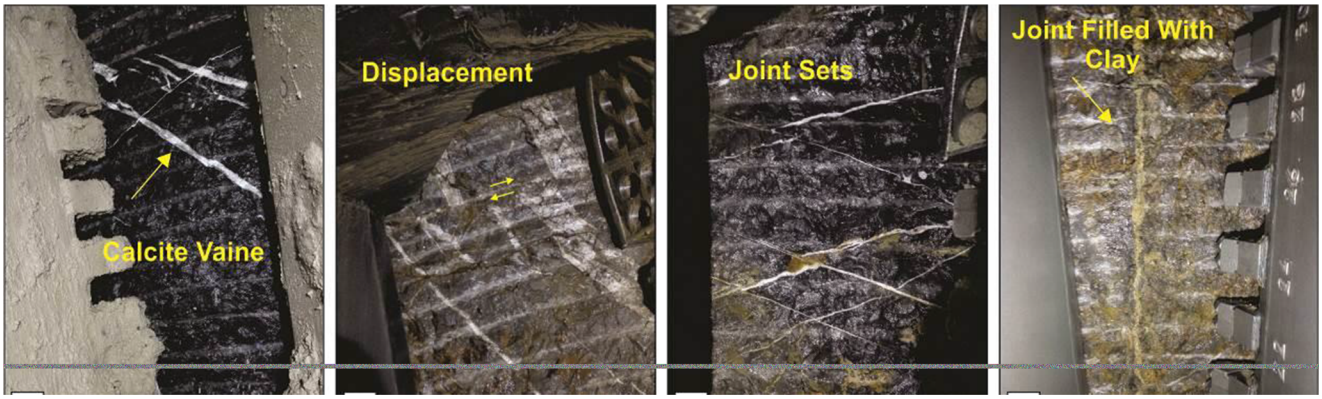


**Fig. 11** The tunnel face mapping and the discontinuity condition in front of the tunnel face

tests (ISRM 1985), which have been carried out both in the job site and in the rock mechanics laboratory. The statistical description and descriptive statistical analysis of UCS values in the database are shown in Fig. 13b and Table 3, respectively. This figure shows that in the SEL6 tunnel, the UCS range varied from 70 MPa to 110 MPa.

## Rock mass parameters

During the visiting and mapping of tunnel face, the collected data have been employed to identify the quality class of limestone rock masses. In this study, the rock mass, encountered at the tunnel face, has been classified according to the RQD and GSI (Hoek et al. 1998; Marinos and Hoek 2001; Marinos et al. 2005; Marinos 2019). Distribution curves and frequency histograms of RQD and GSI data are shown in Fig. 13c, d, respectively. As shown in Fig. 13c, the resulting RQD values range from 60 to 100. According to RQD index, the limestone is mostly characterized by fair to excellent rock quality. Furthermore, as presented in Fig. 13d., the surrounding rock mass of the tunnel face, which is composed of limestone, according to GSI is mainly classified as massive to very blocky (GSI = 40–85). Also, the descriptive statistical analysis of RQD and GSI is presented in Table 3.

## TBM performance in the field

During excavation, all machine operating parameters have been extracted directly from the TBM acquisition system and recorded on a computer connected to the control system via a local connection that allowed calculating the operating and TBM performance parameters. As a result of using logged data, the penetration, total gross thrust, cutter load, RPM, and torque were computed.

According E. Farrokh et al. (2012), a big problem for shielded TBMs, the same with this project, is that the Fn (disc cutter normal force) value used in the predictive calculation is a gross value and does not include any friction losses. The net cutter force (Fn) delivered to the cutterhead may be significantly less than the nominal cutter load calculated from the applied TBM thrust. Therefore, in this study, to determine Fn, the friction losses are subtracted from the TBM thrust.

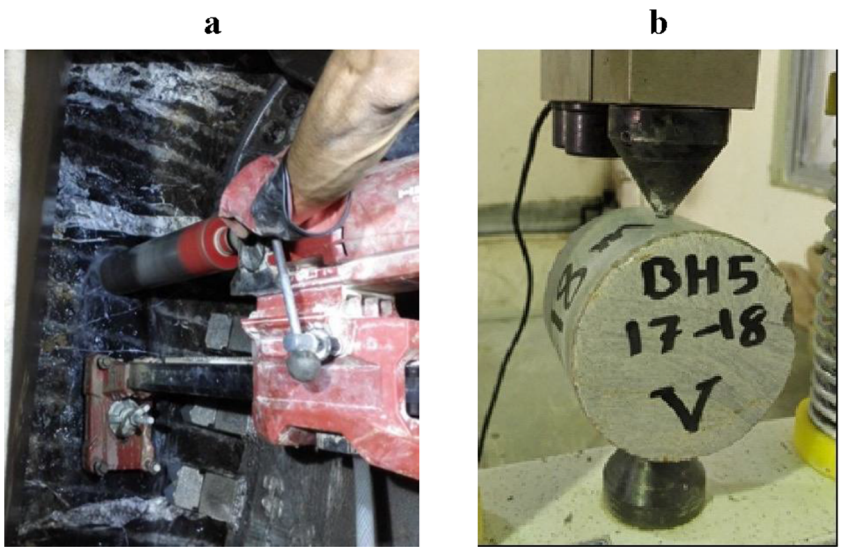


**Fig. 12** **a** Drilling and taking the core rock samples during tunnel face mapping and **b** point load test (PLT)

**Table 3** Descriptive statistics of various parameters in the database

| Parameters | UCS (MPa) | Prev (mm/rev) | Fn (kN) | GSI | Alpha | RQD |
|---|---|---|---|---|---|---|
| Mean | 91.93 | 2.76 | 118.80 | 60.85 | 54.29 | 82.27 |
| Median | 91 | 2.74 | 117.64 | 60 | 55 | 82 |
| Standard deviation | 11.89 | 0.74 | 10.73 | 11.23 | 10.89 | 11.76 |
| Sample variance | 141.37 | 0.55 | 115.16 | 126.13 | 118.56 | 138.25 |
| Kurtosis | −0.89 | −0.80 | −0.49 | −0.46 | −1.13 | −1.34 |
| Skewness | 0.15 | 0.11 | 0.34 | 0.32 | −0.13 | 0.07 |
| Range | 42 | 2.79 | 44 | 45 | 37 | 38 |
| Minimum | 71 | 1.36 | 98 | 40 | 35 | 62 |
| Maximum | 113 | 4.15 | 142 | 85 | 72 | 100 |

A general review of previous prediction performance models, presented in Table 1, shows that depending on the analytical strategy adopted, different objective penetration parameters were employed to aid the prediction of the TBM performance. Usually, the models predict performance parameters such as PR (penetration rate in m/h) and PRev

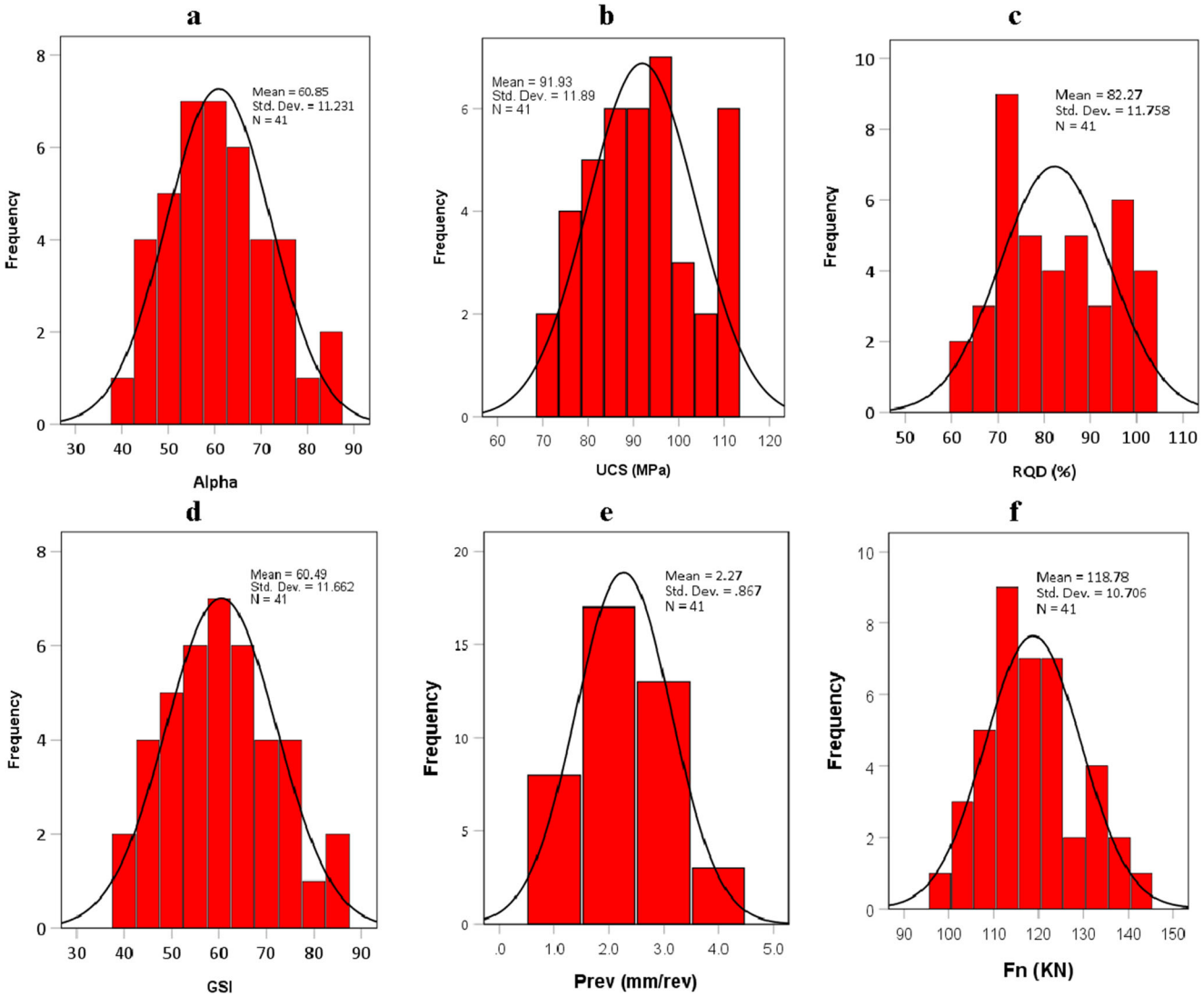


**Fig. 13** Distribution curve and frequency histogram of variation of various parameters in the database. **a** α (alpha angle), **b** UCS, **c** RQD, **d** GIS, **e** PRev, and **f** Fn

**Table 4** The database obtained by engineering geological field investigation and analysis of TBM operation parameters

| No | Ring number | Alpha angle (α) | UCS (MPa) | RQD (%) | GSI | Fn (kN) | PRev (mm/rev) |
|---|---|---|---|---|---|---|---|
| 1 | 501 | 60 | 87 | 89 | 65 | 125 | 3.40 |
| 2 | 502 | 72 | 73 | 88 | 50 | 127 | 3.68 |
| 3 | 510 | 69 | 75 | 66 | 40 | 135 | 4. |
| 4 | 520 | 69 | 101 | 88 | 60 | 120 | 2.78 |
| 5 | 538 | 62 | 97 | 95 | 60 | 102 | 2.17 |
| 6 | 542 | 58 | 90 | 95 | 70 | 112 | 3.12 |
| 7 | 546 | 69 | 95 | 100 | 85 | 110 | 1.92 |
| 8 | 548 | 59 | 110 | 82 | 75 | 109 | 1.55 |
| 9 | 550 | 69 | 106 | 92 | 65 | 117 | 1.99 |
| 10 | 555 | 55 | 97 | 100 | 70 | 122 | 2.81 |
| 11 | 559 | 68 | 89 | 83 | 75 | 117 | 2.29 |
| 12 | 563 | 66 | 84 | 75 | 55 | 114 | 2.92 |
| 13 | 569 | 64 | 88 | 83 | 60 | 123 | 3.09 |
| 14 | 580 | 67 | 100 | 96 | 60 | 114 | 1.93 |
| 15 | 589 | 66 | 88 | 70 | 60 | 112 | 2.54 |
| 16 | 591 | 62 | 85 | 74 | 65 | 133 | 3.47 |
| 17 | 607 | 64 | 102 | 96 | 75 | 120 | 2.07 |
| 18 | 610 | 65 | 89 | 94 | 45 | 129 | 2.93 |
| 19 | 615 | 55 | 74 | 71 | 60 | 140 | 4.0 |
| 20 | 618 | 52 | 98 | 95 | 85 | 125 | 2.74 |
| 21 | 626 | 53 | 94 | 98 | 80 | 112 | 1.83 |
| 22 | 631 | 56 | 82 | 86 | 70 | 122 | 3.23 |
| 23 | 639 | 51 | 91 | 75 | 45 | 108 | 2.62 |
| 24 | 650 | 48 | 97 | 100 | 60 | 115 | 2.58 |
| 25 | 655 | 40 | 112 | 100 | 70 | 108 | 1.36 |
| 26 | 665 | 53 | 110 | 94 | 65 | 122 | 2.37 |
| 27 | 674 | 47 | 78 | 73 | 50 | 118 | 3.50 |
| 28 | 675 | 46 | 81 | 75 | 50 | 105 | 2.70 |
| 29 | 676 | 35 | 113 | 73 | 75 | 98 | 1.66 |
| 30 | 681 | 35 | 82 | 73 | 45 | 103 | 2.44 |
| 31 | 718 | 50 | 71 | 62 | 55 | 142 | 4. |
| 32 | 725 | 48 | 96 | 64 | 65 | 133 | 3.20 |
| 33 | 751 | 47 | 93 | 85 | 55 | 134 | 3.46 |
| 34 | 774 | 42 | 81 | 70 | 55 | 118 | 3.39 |
| 35 | 809 | 46 | 75 | 68 | 50 | 125 | 3.03 |
| 36 | 890 | 35 | 109 | 80 | 65 | 111 | 1.80 |
| 37 | 911 | 42 | 92 | 73 | 55 | 111 | 2.39 |
| 38 | 926 | 55 | 84 | 76 | 50 | 137 | 3.75 |
| 39 | 947 | 42 | 106 | 78 | 55 | 108 | 2.32 |
| 40 | 954 | 40 | 112 | 73 | 55 | 114 | 2.09 |
| 41 | 964 | 44 | 82 | 65 | 45 | 120 | 3.56 |

(penetration per cutterhead revolution). Other indexed parameters employed in some of the empirical prediction models include specific penetration (SP inverse of FPI) and Field Penetration Index (FPI) all of which represent the ease or difficulty of rock mass boring. A more comprehensive description of different objective penetration parameters can be found in the study of E. Farrokh et al. (2012). Meanwhile, for the development of alternative models in grinding conditions, PRev and Fn (cutter load) can be used in statistical studies to allow for an analysis of the real relationship between the various parameters. Variations of measured cutterhead penetration (PRev) and cutter load (Fn) at each sampling point

**Table 5** Summary results of the determination of regression coefficients of the engineering geological and operating parameters with measured PRev

| Parameter | Regression coefficients ($R^2$) | Regression type | Empirical relationship |
|---|---|---|---|
| Fn (kN) | 0.61 | PRev = 0.05Fn - 3.6 | Linear |
| UCS (MPa) | 0.67 | PRev = $15.8e^{-0.02UCS}$ | Exponential |
| RQD (%) | 0.23 | PRev = -0.03RQD + 5.22 | Linear |
| GSI | 0.26 | PRev = -0.03GSI + 4.81 | Linear |
| Alpha angle ($\alpha$) | 0.13 | PRev = $-0.0002\alpha^2 + 0.25\alpha - 4.02$ | Quadratic |

through the tunnel are shown as two distribution curves and frequency histograms in Fig. 13e, f, respectively. Also, the descriptive statistical analysis of TBM performance parameters is presented in Table 3.

Finally, in this study, after extensive data collection in SEL6 tunnel, to perform the analyses for predicting the PRev in grinding condition, a database including engineering geological properties of rock masses and the corresponding TBM operating parameters was established. The data set for each selected ring is shown in Table 4. It must be emphasized that in all 41 selected rings, reliable engineering geological data were available and grinding condition was dominant in boring process.

## Development of new empirical equation for grinding condition

TBM performance depends on both engineering geological (intact rock/rock mass) properties and the operational parameters of the machines (Armetti et al. 2018). In this study, two different objective parameters were used to develop a new model for the estimation of the TBM penetration under a given set of encountered ground conditions in the limestone where the grinding is the dominant phenomenon. In rock engineering practices, the statistical-based empirical equations have been extensively employed to predict a required parameter from some simple tests or available collected data (Gunsallus and Kulhawy 1984; Yagiz 2008). After the establishment of the database (presented in Table 4), one of the commercial software packages for standard statistical analysis (SPSS) was employed to perform the stepwise and multiple variable regression analyses between engineering geological, operating, and performance parameters. The statistical procedure employed in this study included three steps. At the first step, the bivariate analyses between the cutterhead penetration and other parameters are required for identifying influential parameters. After that, the second step included multiple regression analyses to develop the best-fit combination of key parameters that demonstrate the best statistically significant and strongest correlation to PRev. Finally, the prediction capability of the new empirical model was verified using the testing database information.

### The simple and bivariate analyses

To obtain the correlations between engineering geological properties (UCS, Alpha, RQD, and GSI) and TBM operating parameter (Fn), as dependent variables, and actual measured Prev, as independent one, stepwise statistical analyses were carried out and the effect of each engineering geological properties and TBM operating parameters on the Prev was assessed. Figure 14 depicts the correlation between independent variables and cutterhead penetration (PRev). The results of the stepwise regression analysis and obtained equations between the PRev and each independent variable are also summarized in Table 5. As shown in Fig. 14 and Table 5, among the independent variables, UCS and Fn show good correlations with PRev ($R^2 > 0.61$), whereas the quadratic relation between the alpha angle ($\alpha$) and PRev is found very weak with a correlation coefficient ($R^2$) of 0.13.

To investigate the effect of the TBM thrust force on the penetration, the cutter load (Fn) is employed in this study, and the relationship between the PRev and Fn was achieved with an $R^2$=0.61 which is presented in Table 5. As can be seen in Fig. 14a, PRev is a maximum at higher Fn levels. As Fn values increase, PRev values also increase.

In accordance with precedent studies (Graham and PC 1976; Farmer and Glossop 1980; Gong and Zhao 2009; Hassanpour et al. 2011; Armetti et al. 2018), the intact rock strength is related to TBM penetration with an exponential relationship. By increasing the UCS values, the PRev values decrease. According to statistical analysis, an exponential relationship between UCS with the PRev was found good with a correlation coefficient ($R^2$) of 0.67 as demonstrated in Fig. 14b and its empirical equation relating them is also presented in Table 5.

Also, among rock classification parameters (RQD and GSI), as shown, GSI shows a bit better correlation than RQD. Figure 14c, d shows the results of correlating PRev

**Fig. 14** Correlation between independent variables and measured penetration. **a** Fn-PRev, **b** UCS-PRev, **c** RQD-PRev, **d** GSI-PRev, and **e** alpha-PRev

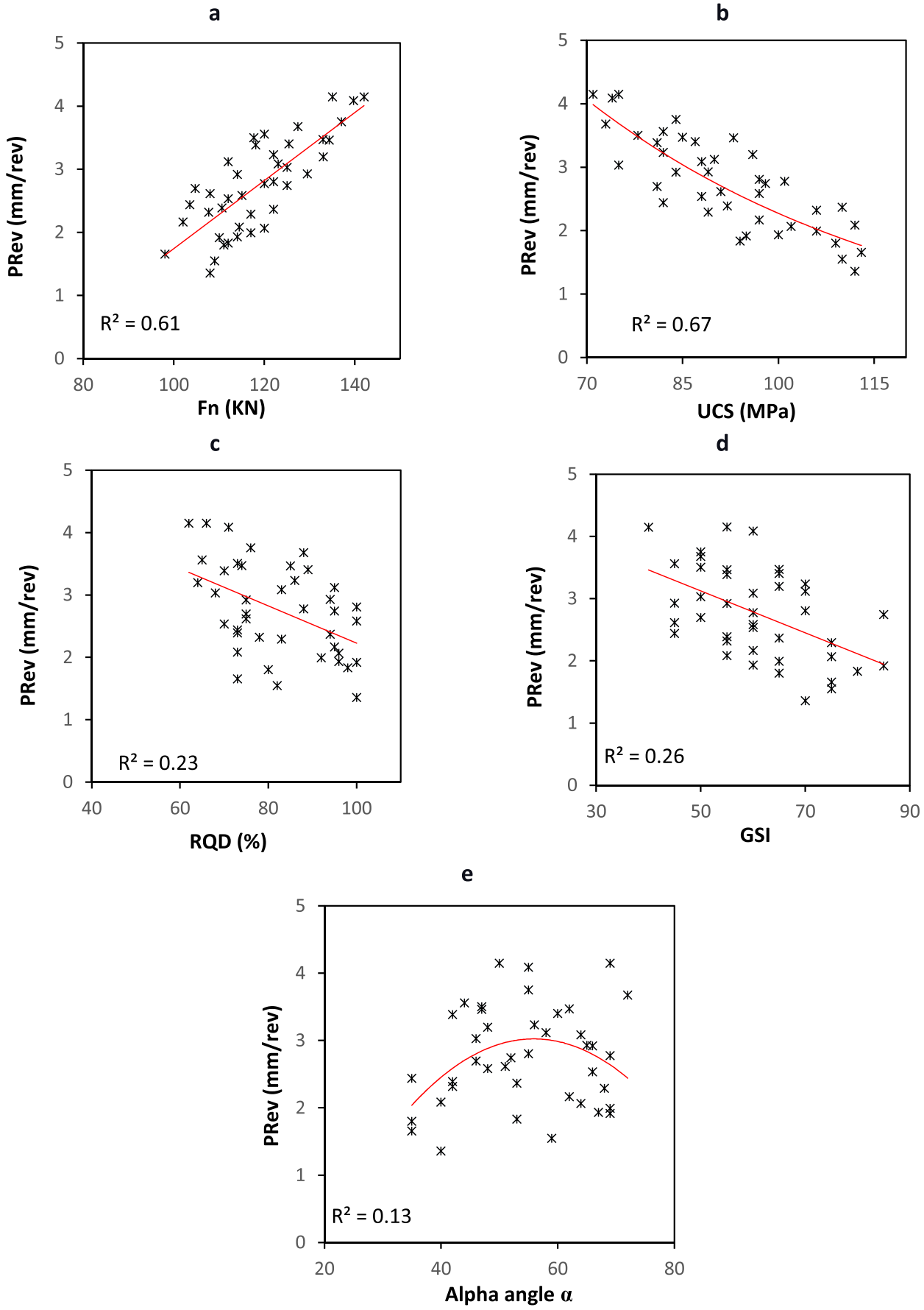
a
PRev (mm/rev)
Fn (KN)
R² = 0.61
b
PRev (mm/rev)
UCS (MPa)
R² = 0.67
c
PRev (mm/rev)
RQD (%)
R² = 0.23
d
PRev (mm/rev)
GSI
R² = 0.26
e
PRev (mm/rev)
Alpha angle α
R² = 0.13

**Table 6** Summary of the generated models for forward stepwise regression analysis

| Model | *R* | *R* square | Adjusted *R* square | Std. error of the estimate |
|---|---|---|---|---|
| 1 | .82[a] | .67 | .66 | .42825 |
| 2 | .93[b] | .86 | .85 | .28603 |
| 3 | .94[c] | .88 | .87 | .26794 |

[a] Predictors: (constant), UCS

[b] Predictors: (constant), UCS, Fn

[c] Predictors: (constant), UCS, Fn, GSI

and RQD and GSI, respectively. RQD is only based upon the discontinuity spacing, whereas GSI value is estimated by two of the main rock mass parameters, including the structure and the condition of the discontinuity surfaces, so the developed equation shows a reasonable correlation between the PRev and GSI rather than RQD. The empirical equation relating the GSI, RQD, and TBM penetration is presented in Table 5.

## Multivariate regression analysis

As mentioned before, in this study, to find an empirical equation and describe the relationships between multiple the independent variables (Fn as the operational parameter and USC, alpha angle (α), RQD, and GSI as engineering geological properties) and dependent variable (PRev), a multiple regression model with a 95% confidence level was used by considering linear functions as follows:

$$Y = \beta_0 + \beta_1 x_1 + \beta_2 x_2 + \ldots + \beta_n x_n, \quad (2)$$

where $Y$ is the dependent variable, $\beta_0$ is a constant value, where the regression line intercepts the $Y$-axis, $x_1$ to $x_n$ are the independent variables, and $\beta_1$ to $\beta_n$ are regression coefficients for $x_1$ to $x_n$, respectively.

Multiple regression analyses, including the significance of the regression coefficients of correlation and the significance of the regressions, were applied using the SPSS software. The influence of each independent variable on PRev was evaluated using forward stepwise regression analyses which can generate different models with input variables as shown in Table 6. In these models, the maximum determination coefficient ($R^2$ = 0.88) and the maximum correlation coefficient ($R$=0.94) were obtained in model 3, which selected Fn, UCS, and GSI as input variables.

To test the significance of the regressions, the analysis of variance ($F$ test) was conducted. The $F$ test results, named ANOVA for the generated different models, are presented in Table 7. All models have different tabulated Fischer index values ($F$ values), since all of them have different numbers of independent variables. According to this rule, when the computed $F$ value is greater than the tabulated $F$ value, there is a real and significant relationship between a dependent (actual PRev) and independent variables (UCS, GSI, and Fn) for generated model. The statistical values $F$ value and level of significance (Sig.) of model 3 are 114.366 and 0.000, respectively. Therefore, the null hypothesis can be rejected, which means that at least one of the independent variables can significantly affect PRev.

Furthermore, the significance of the coefficient of correlation ($R$ values) was determined by the $t$ test, and their results for the generated models are presented in Table 8. The $t$ test shown in Table 8 indicates that the coefficients of model 2 are true. Therefore, in this study, there is a significant linear relationship between independent variables (UCS and Fn) and dependent (actual PRev) in the third model.

Dependent variable: PRev

Consequently, based on the statistical analysis, the correlations obtained between the variables are linear functions, and it appears that the best results could be obtained by excluding the two parameters of alpha angle and RQD. The results show the best-fit regression between PRev as response parameter and

**Table 7** Analysis of variance (ANOVA) for the significance of regression for each generated model

| Model | | Sum of squares | df | Mean square | *F* | Tabulated *F* | Sig. |
|---|---|---|---|---|---|---|---|
| 1 | Regression | 14.670 | 1 | 14.670 | 79.98 | 4.08 | .000[b] |
| | Residual | 7.153 | 39 | .183 | | | |
| | Total | 21.822 | 40 | | | | |
| 2 | Regression | 18.713 | 2 | 9.357 | 114.36 | 3.23 | .000[c] |
| | Residual | 3.109 | 38 | .082 | | | |
| | Total | 21.822 | 40 | | | | |
| 3 | Regression | 19.166 | 3 | 6.389 | 88.98 | 2.84 | .000[d] |
| | Residual | 2.656 | 37 | .072 | | | |
| | Total | 21.822 | 40 | | | | |

[a] Dependent variable: PRev

[b] Predictors: (constant), UCS

[c] Predictors: (constant), UCS, Fn

[d] Predictors: (constant), UCS, Fn, GSI

**Table 8** Multivariate regression coefficients and excluded variables from each generated model

| Model | | Unstandardized coefficients | | Standardized coefficients | *t* | Sig. |
|---|---|---|---|---|---|---|
| | | B | Std. error | Beta | | |
| 1 | (Constant) | 7.440 | .528 | −.820 | 14.097 | .000 |
| | UCS | −.051 | .006 | | −8.944 | .000 |
| 2 | (Constant) | 1.932 | .859 | −.570 | 2.250 | .030 |
| | UCS | −.035 | .004 | | −8.047 | .000 |
| | Fn | .034 | .005 | .498 | 7.030 | .000 |
| 3 | (Constant) | 1.983 | .805 | −.479 | 2.463 | .019 |
| | UCS | −.030 | .005 | | −6.333 | .000 |
| | Fn | .035 | .005 | .510 | 7.669 | .000 |
| | GSI | −.011 | .004 | −.168 | −2.511 | .017 |

UCS and Fn predictors, in a linear combination with a 95% confidence level. As a result, new performance predictive equation in grinding condition was empirically obtained as a function of measured engineering geological properties and operational parameter in the model 3 as illustrated in Tables 6, 7, and 8, as follows:

$$\mathrm{PRev} = 1.98 + 0.035\mathrm{Fn} - 0.03\mathrm{UCS} - 0.011\mathrm{GSI}, \quad (3)$$

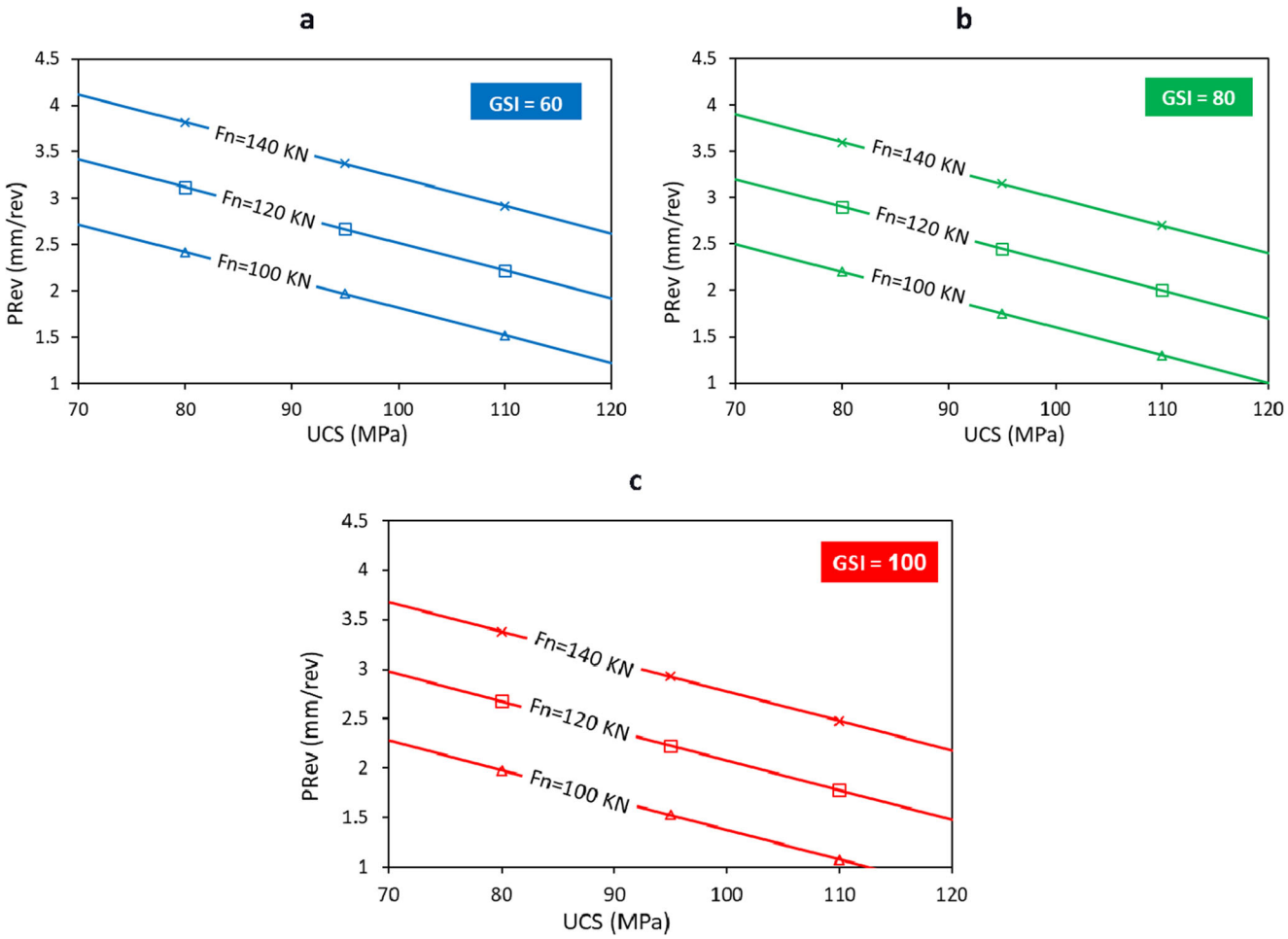


**Fig. 15** Chart for estimating PRev in limestone rocks based on UCS and Fn in grinding condition for different GSI values. **a** GSI=60, **b** GSI=80, and **c** GSI=100

**Table 9** The RMSE values calculated for the model developed in this study and selected prediction models

| Row | Prediction models | RMSE value |
|---|---|---|
| 1 | Graham (1976) | 2.49 |
| 2 | Hassanpour et al. (2015) | 1.73 |
| 3 | Farrokh et al. (2012) | 4.52 |
| 4 | The developed model in this study | 0.26 |

where PRev is in mm/rev, UCS is in MPa, and Fn is disc cutter normal force in kN.

Moreover, a penetration prediction chart for grinding condition from Eq. (3) is developed and shown in Fig. 15 for convenient and practical application. The approximate range of PRev can be estimated quickly using Fig. 15 in limestone rocks with different UCS and Fn values for different GSI values. However, it must be emphasized that the influences of the rock mass classification systems (GSI and RQD) and alpha angle on the penetration are not significant in the developed model, statistically.

## Verification of the developed model

To evaluate the accuracy of the developed model in this study and also some existing prediction models (Graham 1976; Hassanpour et al. 2015; Farrokh et al. 2012), the measured penetration per revolution (PRev) is compared with the

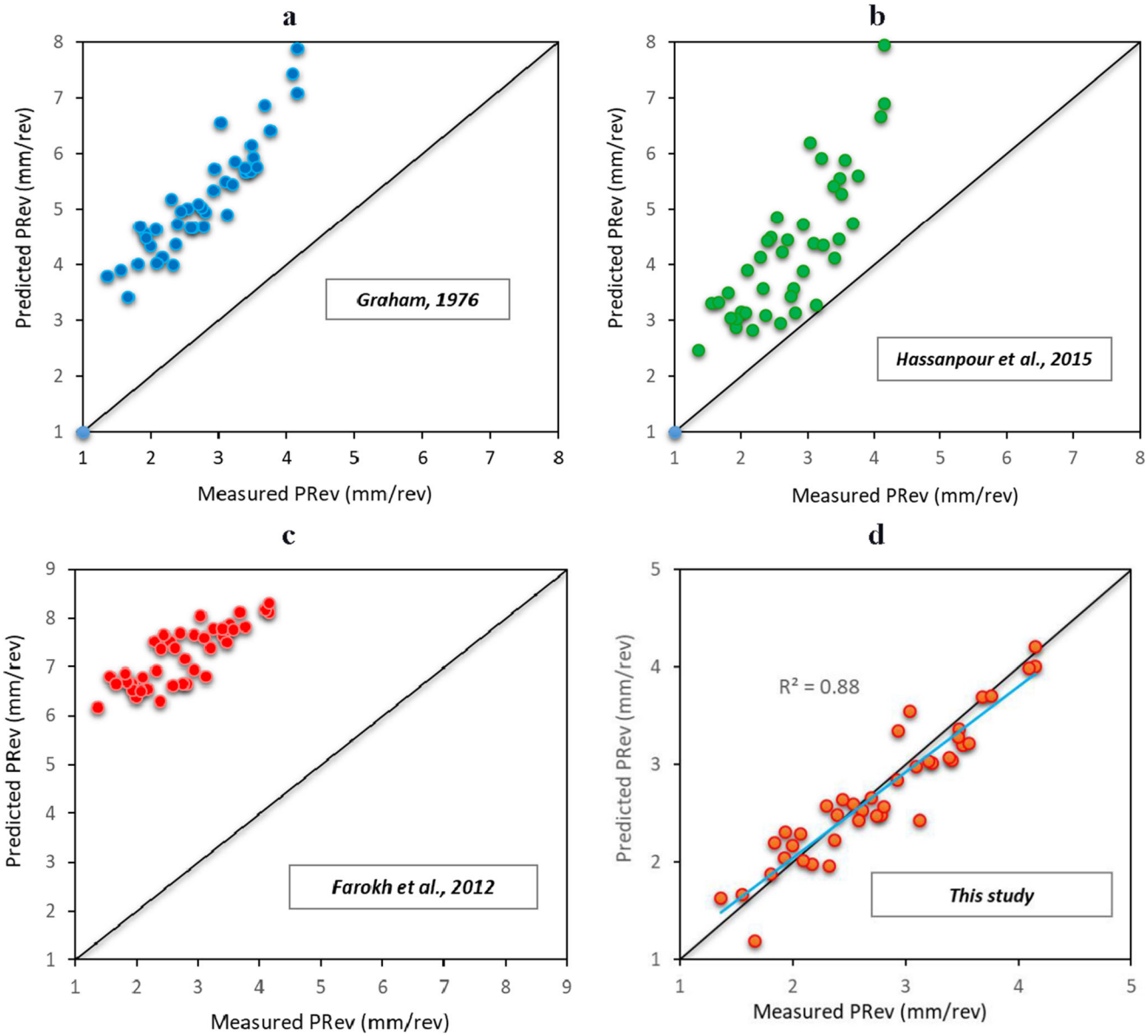


**Fig. 16** Comparison of measured and predicted penetrations (PRev) using the developed model in this study and selected prediction models. **a** Graham (1976) model, **b** Hassanpour et al. (2015) model, **c** Farrokh et al. (2012) model, and **d** the model developed in this study

predicted one in each sampling point throughout the tunnel. The measured and predicted values of the PRev are compared in Fig. 16. Moreover, to verify the performance of the developed model and some existing prediction models, root mean square error (RMSE) (Eq. 4) and $R^2$ (coefficient of determination) parameters are employed in this study and also presented in Table 9. RMSE is a measure of how concentrated the data is around the line of best fit. Statistically, a perfect model with excellent predictability can achieve $R^2$ and RMSE values of 1 and 0, respectively. Furthermore, lower RMSE values refer to lower errors and better performance of the proposed model.

$$\mathrm{RMSE} = \sqrt{\frac{1}{n}\sum_{i=1}^{n}\left(z_i - \hat{z}_i\right)^2}, \tag{4}$$

where $z_i$ is the real value, $\hat{z}_i$ is the predicted value, and $n$ is the number of data points. As shown in Fig. 16 and Table 9, the $R^2$ value and RMSE of the developed model in this study were obtained 0.8 and 0.26 respectively, whereas the RMSE value of existing prediction models, Graham 1976, Hassanpour et al. 2015, and Farrokh et al. 2012, were measured 2.49, 1.73, and 4.25 respectively, which indicate that the developed model in this study has an acceptable accuracy level in predicting TBM PRev in grinding conditions. Also, the predicted values by this model are quite close to the actual ones, and most of the ΔPRev values (the difference between PRev predicted using Eq. (3) and the measured PRev) are less than 0.5 mm/rev. In general, the higher accuracy of the proposed model shows the potential for a more accurate prediction of cutterhead penetration for grinding conditions in limestone strata and low cutter load. Further study of this approach depends on the establishment of new databases that incorporate additional mechanized tunneling projects and engineering geological factors.

## Conclusion

The geotechnical and engineering geological surveys during excavation of SEL6 tunnel allowed subdividing the tunnel into two distinct geological formations including Tehran alluviums and strong Cretaceous limestone. This research has focused on TBM performance in limestone strata. In a major part of these limestone rocks, due to machine limitations, excavation was carried out on grinding-dominated mode. In fact, in these parts of tunnel, cutterhead penetration was usually less than 4 mm/rev.

In this study, based on the rock cutting process, the engineering geological properties influencing TBM performance were identified, firstly. Then, four rock mass parameters, namely, UCS, alpha angle, RQD, and GSI, and one operational TBM parameter named Fn were chosen to evaluate machine performance in selected tunnel sections in limestone strata where grinding phenomenon was dominant. Then, a comprehensive database which includes rock mass properties, operating parameters of machine, and TBM performance parameters were developed. By analyzing the face mappings and screening the rock test results, a total of 41 data sets with reliable data were selected. By using multiple variable linear regression analyses, a prediction model was proposed to evaluate TBM performance range for the grinding conditions.

The comparison between rock properties and TBM indices showed that UCS, GSI, and Fn affect the TBM penetration more effectively than other parameters. It was also shown that the uniaxial compressive strength of intact rock (UCS) and the geological strength index (GSI) have been successfully considered to estimate the boreability of a given rock formation where grinding occurs.

Also, the proposed empirical relationship in this article should be considered valid only for new projects with similar engineering-geological conditions and TBM specifications. Further research should be done to investigate the effect of engineering geological properties on TBM performance, and more field data from different mechanized projects need to be collected to develop a universal model that can be applied to other lithologies and TBM specifications.

**Acknowledgments** The authors wish to thank Tehran Metro Co. and Rahsaz-Tarh Consulting Engineering (RTCE) Co. for permission to publish the information contained in this paper. The authors thank especially Dr. Sadegh Tarigh Azali, Mr. Alireza Amiri, and Dr. Emad Khorasani for reviewing the content of the paper and valuable commenting.

## References

Armetti G, Migliazza MR, Ferrari F et al (2018) Geological and mechanical rock mass conditions for TBM performance prediction. The case of "La Maddalena" exploratory tunnel, Chiomonte (Italy). Tunn Undergr Sp Technol 77:115–126

Balci C, Bilgin N (2007) Correlative study of linear small and full-scale rock cutting tests to select mechanized excavation machines. Int J Rock Mech Min Sci 44:468–476

Berdal T, Jakobsen PD, Jacobsen S (2018) Utilising excavated rock material from tunnel boring machines (TBMs) for concrete. SynerCrete' 8 International Conference on Interdisciplinary Approaches for Cement-based Materials and Structural Concrete, Funchal, Madeira Island, Portugal.

Brino G, Peila D, Steidl A, Fasching F (2015) Prediction of performance and cutter wear in rock TBM: application to Koralm tunnel project. GEAM-GEOINGEGNERIA Ambient E MINERARIA-GEAM-GEOENGINEERING. Environ Min:37–50

Bruland A (1998) Hard rock tunnel boring, vol 1–10

Delisio A, Zhao J, Einstein HH (2013) Analysis and prediction of TBM performance in blocky rock conditions at the Lötschberg Base Tunnel. Tunn Undergr Sp Technol 33:131–142

Farmer IW, Glossop NH (1980) Mechanics of disc cutter penetration. Tunnels Tunn 12:22–25

Farrokh E, Rostami J, Laughton C (2012) Study of various models for estimation of penetration rate of hard rock TBMs. Tunn Undergr Sp Technol 30:110–123

Firouzei Y, Hassanpour J, Pourhashemi SM (2019) Tunneling with a soft rock EPB machine in hard rock conditions, the experience of Tehran metro line 6 southern expansion sector. In: 4th International Conference on Tunnel Boring Machines in Difficult Grounds. Denver, USA

Frenzel C, Galler R, Käsling H, Villeneuve M (2012) Penetration tests for TBMs and their practical application/Penetrationstests für Tunnelbohrmaschinen und deren Anwendung in der Praxis. Geomech Tunn 5:557–566

Frenzel C, Käsling H, Thuro K (2008) Factors influencing disc cutter wear. Geomech Tunnelbau Geomech Tunnelbau 1:55–60

Gong Q, Zhao J (2009) Development of a rock mass characteristics model for TBM penetration rate prediction. Int J Rock Mech Min Sci 46:8–18

Graham PC, PC G (1976) Rock exploration for machine manufacturers.

Gunsallus KL, Kulhawy FH (1984) A comparative evaluation of rock strength measures. In: International Journal of Rock Mechanics and Mining Sciences & Geomechanics Abstracts. Elsevier, Amsterdam, pp 233–248

Hassanpour J, Rostami J, Zhao J (2011) A new hard rock TBM performance prediction model for project planning. Tunn Undergr Sp Technol 26:595–603

Hassanpour J, Rostami J, Zhao J, Tarigh Azali S (2015) TBM performance and disc cutter wear prediction based on ten years' experience of TBM tunneling in Iran. Geomech Tunnelbau 8(3):239–247

Hassanpour J, Firouzei Y, Hajipour G (2020) Actual performance analysis of a double shield TBM through sedimentary and low to medium grade metamorphic rocks of Ghomrood Water Conveyance Tunnel Project (Lots 3 & 4). Bull Eng Geol Environ, **under production**. https://doi.org/10.1007/s10064-020-01947-z

Hoek E, Marinos P, Benissi M (1998) Applicability of the Geological Strength Index (GSI) classification for very weak and sheared rock masses. The case of the Athens Schist Formation. Bull Eng Geol Environ 57:151–160

ISRM (1978) Suggested methods for the quantitative description of discontinuities in rock masses. Int J Rock Mech Min Sci Geomech Abstr 15:319–368

ISRM (1985) Suggested method for determining point load strength. Int J Rock Mech Min Sci Geomech Abstr 22:51–60

Koopialipoor M, Tootoonchi H, Armaghani DJ et al (2019) Application of deep neural networks in predicting the penetration rate of tunnel boring machines. Bull Eng Geol Environ 78:6347–6360

Labra C, Rojek J, Onate E (2017) Discrete/finite element modelling of rock cutting with a TBM disc cutter. Rock Mech Rock Eng 50:621–638

Lazemi HA, Dehkordi MS (2019) Estimation of the TBM penetration rate using the post-failure behavior of a rock mass and the equivalent thrust per cutter. A case study: the Amirkabir Water Transferring Tunnel of Iran. Bull Eng Geol Environ 78:1735–1746

Marinos P, Hoek E (2001) Estimating the geotechnical properties of heterogeneous rock masses such as flysch. Bull Eng Geol Environ 60:85–92

Marinos V (2019) A revised, geotechnical classification GSI system for tectonically disturbed heterogeneous rock masses, such as flysch. Bull Eng Geol Environ 78:899–912

Marinos V, Marinos P, Hoek E (2005) The geological strength index: applications and limitations. Bull Eng Geol Environ 64:55–65

Rahsaz-Tarh Consulting Engineers (2016) Engineering geological investigation report of Southern Extension of Tehran Metro Line, p 6

Salimi A, Rostami J, Moormann C, Hassanpour J (2018) Examining feasibility of developing a rock mass classification for hard rock TBM application using non-linear regression, regression tree and generic programming. Geotech Geol Eng 36(2):1145–1159

Tarigh Azali S, Ghafoori M, Lashkaripour GR, Hassanpour J (2013) Engineering geological investigations of mechanized tunneling in soft ground: a case study, East–West lot of line 7, Tehran Metro, Iran. Eng Geol 166:170–185

Tarigh Azali S, Pourhashemi SM, Khorasani E (2018) NATM Tunneling in urban area, a review of planning, executing, and monitoring in Tehran Metro Line 6. In: ITA - AITES WORLD TUNNEL CONGRESS (WTC 2018). Dubai

Villeneuve M (2008) Examination of geological influence on machine excavation of highly stressed tunnels in massive hard rock

Villeneuve MC (2017) Hard rock tunnel boring machine penetration test as an indicator of chipping process efficiency. J Rock Mech Geotech Eng 9:611–622

Villeneuve MC, Diederichs MS, Kaiser PK (2012) Effects of grain scale heterogeneity on rock strength and the chipping process. Int J Geomech 12:632–647

Yagiz S (2008) Utilizing rock mass properties for predicting TBM performance in hard rock condition. Tunn Undergr Sp Technol 23:326–339

Zhou J, Yazdani Bejarbaneh BJA, Danial TMM (2020) Forecasting of TBM advance rate in hard rock condition based on artificial neural network and genetic programming techniques. Bull Eng Geol Environ 79:2069–2084